Quantifying Offset-Dependent Seismic Prestack Data Quality Using Data-Driven Metrics Across Different Acquisition Geometries

Akshika Rohatgi[1], Andrey Bakulin[1], Hassan Odhawani[2], and Sergey Fomel[1], University of Texas at Austin, [2]TGS*

Summary

Land seismic acquisition acknowledges offset-dependent noise, yet acquisition geometries are typically designed with uniform sampling across offsets, with limited quantitative feedback on how prestack data quality varies in practice. Here, we use data-driven metrics to evaluate offset- and frequency-dependent prestack data quality and to compare two 3D surveys acquired over the same subsurface. Using offset-dependent signal-to-noise ratio (SNR) and frequency-dependent phase stability, we apply the same diagnostics consistently to raw and processed data, allowing data quality to be tracked objectively through the processing sequence. The results show that systematic differences persist across offset ranges and frequency bands, demonstrating that prestack data quality can be quantified directly from the data at any stage, enabling unbiased comparison of acquisitions and realistic assessment of processing outcomes.

Introduction

Land seismic acquisition geometry defines how the wavefield is sampled in space, but the character of recorded prestack data is controlled primarily by the source and receiver arrays themselves. Array design determines how signal and noise are summed, attenuated, or preserved at the time of recording (Bakulin et al., 2024), whereas parameters such as receiver spacing, fold distribution, azimuthal coverage, and offset range govern how frequently and how completely that wavefield is sampled and propagated to the final imaging step (Meunier, 2011; Vermeer, 2012; Al Mesaabi, 2021).

On land, it is well understood that near offsets are typically dominated by surface-related noise, while far offsets tend to contain more coherent reflection energy. However, these offset-dependent differences are rarely quantified directly from the data and are not explicitly incorporated into acquisition evaluation or design workflows. Instead, acquisition performance is commonly assessed using geometric descriptors such as offset–azimuth distribution, trace density, or fold, without quantitatively closing the loop to prestack data quality or processing outcomes.

In this study, we address this gap by introducing a data-driven framework for evaluating prestack data quality using consistent, objective metrics derived directly from the data. The same diagnostics are applied to raw field records and final processed prestack volumes, enabling quantitative tracking of how prestack data quality evolves through processing. We combine offset-dependent signal-to-noise ratio (SNR) with frequency-dependent phase variability estimated using circular statistics (Rohatgi et al., 2025), providing complementary measures of signal strength and waveform stability. This framework enables objective comparison of acquisition implementations and provides a transparent, repeatable basis for assessing prestack data quality and strengthening the feedback loop between acquisition and processing.

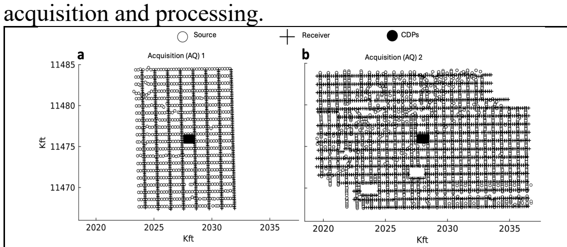

Figure 1: Source–receiver map for CMP supergathers extracted at the same location from two co-located 3D surveys. Symbols show the distribution of shots, receivers, and contributing CDPs for (a) AQ1 and (b) AQ2, providing a 2D view of the sampling and offset/azimuth coverage of each acquisition.

3D Land Seismic Data Sets and Comparison Framework

We analyze two co-located 3D land seismic surveys acquired over the same subsurface region but utilizing different acquisition parameters. The surveys, referred to as Acquisition 1 (AQ1) and Acquisition 2 (AQ2), image identical geology, allowing prestack data quality to be compared without geological ambiguity. Key acquisition parameters are summarized in Table 1. While both surveys use comparable source strength and similar areal coverage, they differ primarily in sampling density and number of geophones per station, with AQ1 using larger receiver arrays than AQ2. For a direct, data-driven comparison, we extracted 8 × 8 CDP supergathers centered at the same subsurface location from both datasets (Figure 1).

Parameters	Acquisition 1	Acquisition 2
Source inline spacing (ft)	220	165
Source crossline spacing (ft)	880	660
Receiver inline spacing (ft)	220	165
Receiver crossline spacing (ft)	1100	990
Patch area (ft^2)	8251 x 16712	16551 x 16148
Geophones per station	6	3

Table 1. Key acquisition parameters for the two surveys

These supergathers represent the actual ensemble of traces contributing to a fixed CMP location and therefore capture how each acquisition samples the wavefield and associated noise across offsets and azimuths. After applying statics and normal moveout (NMO) corrections, traces were sorted by offset to examine offset-dependent behavior under identical subsurface illumination. Both raw and processed data are analyzed. Raw supergathers from both surveys exhibit

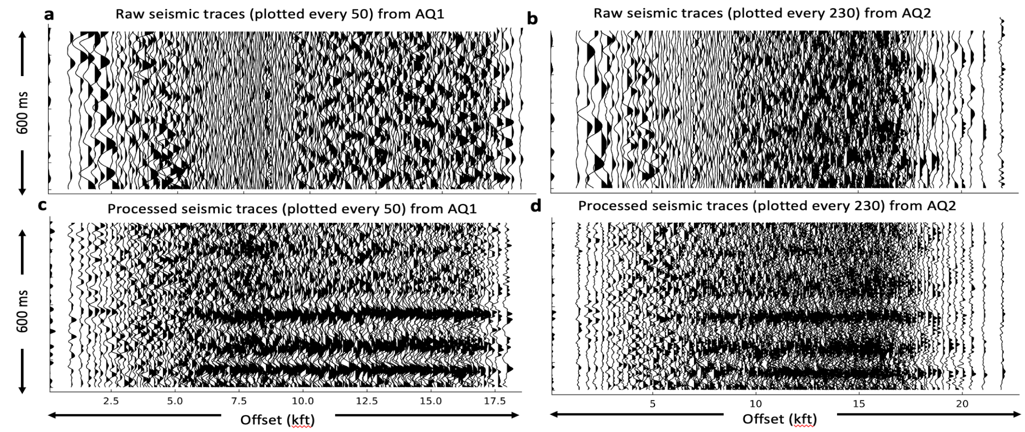

Figure 2: Raw and processed CMP supergathers from two co-located 3D land surveys. Raw gathers from AQ1 (a) and AQ2 (b) and the corresponding processed gathers (c, d) are shown at regular trace intervals as a function of offset.

strong offset-dependent variations in data quality (Figure 2a,b). Near offsets are dominated by coherent surface-related noise, primarily ground roll, which obscures primary reflections, whereas reflection events become increasingly discernible at intermediate to far offsets. This behavior reflects well-known land seismic wave propagation effects, in which surface waves and scattered energy dominate the near-offset region, producing the characteristic noise cone in prestack data.

Processing improves data quality for both surveys (Figure 2c,d), but clear differences persist. In AQ1, coherent reflections emerge at shorter offsets and remain relatively stable across the gather. In contrast, AQ2 exhibits greater waveform variability and stronger noise domination at near offsets, despite usable signal at larger offsets. These effects represent two sides of the same phenomenon: increased waveform instability manifests as reduced coherence and elevated noise. As noted by Bakulin et al. (2024), waveform variability decreases with increasing receiver-array size, consistent with the use of six-geophone arrays in AQ1 compared to three-geophone arrays in AQ2. As a result, prestack data quality remains non-uniform across offsets and differs between surveys even after processing, despite imaging the same subsurface. Visual inspection alone cannot determine how much usable signal each portion of the aperture contributes. To objectively compare how the two acquisitions sample and preserve prestack signal and how these differences evolve through processing, we next quantify data quality using data-driven metrics. Specifically, we compute signal-to-noise ratio (SNR) as a function of offset for both raw and processed datasets.

Offset-Dependent Prestack Data Quality from SNR

We quantify offset-dependent prestack data quality using a data-driven, stack-based SNR metric following Bakulin et al. (2022). SNR is estimated in local time windows after moveout correction, assuming locally flattened and coherent reflection energy. Signal strength is measured from coherently stacked energy, while incoherent energy provides a noise estimate, allowing SNR to be evaluated directly from the data without reliance on geometric proxies. Figure 3 shows SNR versus offset for both surveys in raw and fully processed prestack form. For both datasets, SNR increases with offset, reflecting the well-known dominance of surface-related noise at near offsets and the emergence of more coherent reflection energy at larger offsets.

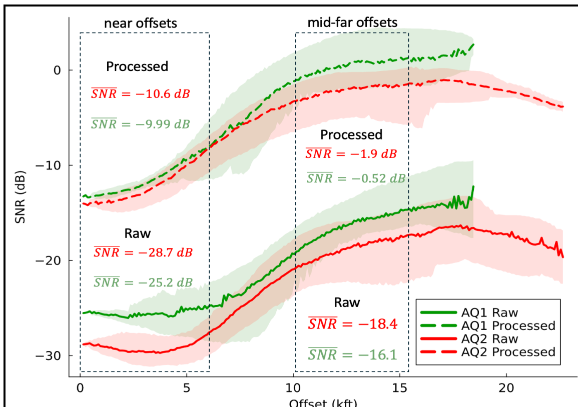

Figure 3. Offset-dependent SNR for raw and processed supergathers from two acquisitions. SNR increases with offset for both surveys, revealing a pronounced near–far offset contrast that persists after processing. Acquisition 1 consistently achieves higher SNR than Acquisition 2 before and after processing, consistent with the use of larger receiver arrays (six vs. three geophones per station). Shaded bands indicate variation due to azimuths.

Near offsets exhibit the lowest SNR values, whereas far offsets show progressively improved signal quality, consistent with the characteristic noise-cone behavior in land seismic data. Processing increases SNR across all offsets for both surveys, but relative differences persist. AQ1 consistently shows higher SNR than AQ2 before and after processing, consistent with the use of six-geophone receiver arrays in AQ1 versus three-geophone arrays in AQ2. Processing does not eliminate the strong near–far offset contrast: for both surveys, near-offset SNR remains more than 10 dB lower than far-offset SNR after processing. This reflects the fundamentally higher noise levels at near offsets rather than differences in processing effectiveness. Because trace density is comparable across offsets, multichannel processing achieves similar relative noise suppression, but the absolute noise level remains much higher at near offsets. As a result, near-offset data do not reach the SNR levels observed at far offsets, highlighting the need for increased sampling or alternative strategies if more uniform prestack SNR is desired. While SNR provides a robust measure of usable signal strength, it does not capture waveform stability. Even in offset ranges with moderate to high SNR, frequency-dependent phase variability can degrade coherence and limit imaging performance. We therefore next examine phase stability using circular statistics to provide complementary, frequency-resolved diagnostics of prestack data quality.

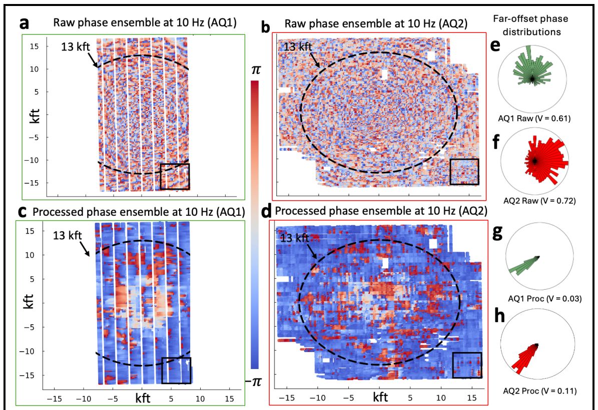

Figure 4. Phase ensembles at 10 Hz extracted from the same subsurface location for the two acquisitions: raw data for AQ1 (a) and AQ2 (b), and corresponding processed data (c, d). (e–h) Far-offset phase distributions from the offset ring (black box), showing higher phase variance for AQ2 in the raw data and reduced but persistently larger variance after processing.

Frequency-dependent phase variability

Near-surface complexity and residual surface-related noise in land seismic data introduce phase distortions that vary with frequency. To quantify this behavior, we analyze phase stability in the frequency domain using CMP supergathers extracted from the two surveys. Figure 4 shows representative phase ensembles at 10 Hz for AQ1 and AQ2. While these ensembles provide qualitative insight into waveform consistency, visual inspection alone is insufficient for objective comparison of phase stability.

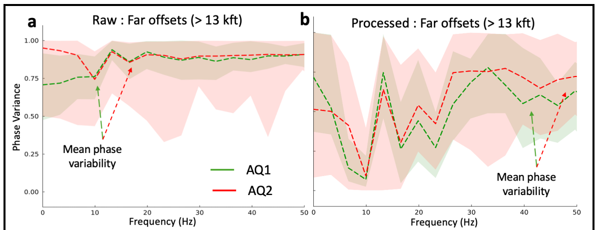

Figure 5. Phase variance (V) versus frequency for far offsets (>13 kft) for two acquisitions: (a) raw data and (b) data after time-domain processing. Processing reduces phase variability across much of the bandwidth, but systematic differences persist. Shaded bands indicate the azimuthal range of phase variance within the offset ring, and dashed curves represent the azimuthal mean.

We quantify phase variability using circular statistics following Rohatgi et al. (2025). Phase dispersion is measured using circular variance, which ranges from 0 to 1, with values near 0 indicating stable, coherent phase (signal-dominated behavior) and values near 1 indicating random, noise-dominated phase. Circular variance therefore provides a direct, data-driven measure of phase coherence, analogous to SNR but focused on waveform stability rather than amplitude. Phase distributions are computed in local time windows from subsets of traces sharing common offsets and azimuths within the CMP supergathers (black boxes in Figure 4), ensuring comparable propagation paths. This windowed approach parallels the local, event-based SNR estimation, enabling phase stability to be evaluated consistently along the same reflection events. Representative phase distributions for far offsets are shown in Figure 4e–h. In the raw data, AQ1 exhibits lower phase variance than AQ2 (V = 0.61 for AQ1 and V = 0.72 for AQ2), indicating more stable phase behavior. After processing, phase variance decreases for both surveys (V = 0.03 for AQ1 and V = 0.11 for AQ2), reflecting suppression of incoherent noise, although AQ2 remains less phase-stable than AQ1. To examine frequency dependence systematically, we compute phase variance across the seismic bandwidth using a sliding-window approach. Within each spatial window, traces sharing common offsets and azimuths are grouped and circular variance is computed for each frequency, producing frequency-resolved maps of phase variability for the reflector of interest. We focus on far offsets and extract an annular offset ring greater than 13 kft (Figure 4), collecting all phase-variance values within this ring. The variance within the ring provides a quantitative measure of phase stability for the corresponding offset range at each frequency. The resulting phase-variability spectra are shown in Figure 5. In the raw data (Figure 5a), phase variability is high across much of the bandwidth, with AQ2 consistently exhibiting larger variance than AQ1, consistent with the waveform distortions observed in Figure 4. After processing (Figure 5b), phase variability decreases for both surveys, but the reduction is frequency dependent. AQ1 achieves lower phase variance over multiple frequency bands, whereas AQ2 retains elevated variability, indicating persistent phase instability. Notably, both surveys exhibit increased phase variance at the low and high ends of the spectrum, suggesting reduced source effectiveness and wavefield coherence at these frequencies. These results demonstrate that, beyond amplitude-based differences captured by SNR, the two surveys differ in frequency-dependent phase stability. Even at comparable offsets, the recorded wavefield exhibits distinct coherence characteristics, reflecting how near-surface effects, residual noise, and wave propagation are sampled and preserved by different receiver-array implementations. The frequency dependence further provides practical insight: stable low-frequency phase behavior is critical for applications such as waveform-based inversion, while high-frequency phase stability is essential for high-resolution imaging.

Metric	Offset	Stage	AQ1	AQ2
SNR (dB)	Near	Raw	**-25.2**	-28.7
		Processed	**-9.99**	-10.6
	Far	Raw	**-16.1**	-18.4
		Processed	**-0.52**	-1.9
Phase Variance (Averaged over all frequencies) (0 = coherent, 1 = incoherent)	Near	Raw	**0.93**	0.96
		Processed	**0.85**	0.89
	Far	Raw	**0.75**	0.79
		Processed	**0.51**	0.57

Table 2. Quantitative comparison of prestack data quality for AQ1 and AQ2 using data-driven metrics. Signal-to-noise ratio (SNR) and phase variance (averaged over all frequencies) are reported for near and far offsets in raw and processed conditions. Processing improves both metrics for both surveys, but AQ1 consistently exhibits higher SNR and lower phase variance than AQ2, reflecting persistent differences in how the wavefield is sampled and preserved.

Table 2 summarizes quantitative prestack data quality metrics for AQ1 and AQ2, combining offset-dependent SNR and frequency-averaged phase variance for near and far offsets in raw and processed conditions. Near offsets consistently exhibit lower SNR and higher phase variance, reflecting stronger surface-related noise contamination, whereas far offsets show higher SNR and more stable phase behavior. Processing improves both metrics for both surveys but does not eliminate offset-dependent contrasts or relative differences between acquisitions. Across all conditions, AQ1 consistently exhibits higher SNR and lower phase variance than AQ2, consistent with the use of larger receiver arrays that more effectively suppress coherent noise and stabilize the phase. Taken together, these results show that while wave propagation and near-surface effects govern the character of the recorded wavefield, acquisition implementation controls how effectively that wavefield can be improved by processing. Receiver arrays influence the raw waveform at the time of recording, whereas trace density governs the achievable uplift in SNR and phase stability across offsets and frequencies during processing. The proposed data-driven metrics make this progression measurable, providing a quantitative basis for linking acquisition decisions to processing outcomes and for improving future survey design.

Conclusions

This study presents a quantitative, data-driven comparison of two co-located 3D land seismic surveys acquired with different acquisition implementations. By combining offset-dependent signal-to-noise ratio with frequency-dependent phase variability, we evaluate prestack data quality using human-independent metrics derived directly from the data, without reliance on geometric proxies or subjective interpretation. The analysis confirms that prestack data quality is strongly offset-dependent. Near offsets are dominated by surface-related noise, resulting in low SNR and high phase variability, whereas far offsets exhibit higher SNR and more stable phase behavior. Conventional processing improves both signal strength and phase coherence for both surveys but does not eliminate these contrasts. Across all conditions, Acquisition 1, which employs larger receiver arrays (six geophones per station), consistently exhibits higher SNR and lower phase variability than Acquisition 2 (three geophones per station), both before and after processing. Importantly, the SNR gap between near and far offsets persists after processing, indicating that processing alone does not compensate for limitations imposed at acquisition. More broadly, the results demonstrate that offset- and frequency-dependent prestack data quality can be quantified objectively using automated, data-driven diagnostics. These metrics can be applied consistently to raw data, intermediate products, and final prestack volumes, and evaluated spatially or volume-wide for specific targets. The analysis reveals that while far-offset data often achieve stable signal levels, near-offset data remain systematically degraded, suggesting that uniform acquisition effort across offsets may be inefficient. As such, the proposed framework provides a practical basis for diagnosing where additional sampling effort is most impactful and for strengthening the feedback loop between acquisition and processing toward more performance-driven survey design.

Acknowledgments

We thank TGS for providing selected datasets used in this study and Justin Simmons and Christopher Egger for helpful guidance.

References

Al Mesaabi, S.A., Cambois G., Cowell, J., Arnold, D., Boukhanfra, M.F., Al Karbi, S.H., Mahgoub, M., and K. Obaid 2021, Lessons Learned From the World's Largest Continuous Onshore and Offshore 3D Seismic Survey: Abu Dhabi International Petroleum Exhibition & Conference, SPE-208009-MS, DOI: https://doi.org/10.2118/208009-MS.

Bakulin, A., I. Silvestrov, 2023, Closing the loop: From acquisition design to image quality: *The Leading Edge*, 42, 846–853, doi:10.1190/tle42110846.1.

Bakulin, A., I. Silvestrov, and M. Protasov, 2022, Signal-to-noise ratio computation for challenging land single-sensor seismic data: Geophysical Prospecting, 70(3), 629–638, doi: 10.1111/1365-2478.13197.

Meunier, J., 2011, Seismic acquisition from yesterday to tomorrow: SEG/EAGE, Distinguished Instructor Series, no. 14, https://doi.org/10.1190/1.9781560802853.

Rohatgi, A., A. Bakulin, and S. Fomel, 2025, Data-driven analysis of seismic phase using circular statistics: The Leading Edge, 44, 683–691, doi: 10.1190/tle44090683.1.

Vermeer, G., 2012, 3D seismic survey design, 2nd edition: SEG, https://doi.org/10.1190/1.9781560803041.